*Open Forum Infectious Diseases*

MAJOR ARTICLE

# Increased Capsule Thickness and Hypermotility Are Traits of Carbapenem-Resistant *Acinetobacter baumannii* ST3 Strains Causing Fulminant Infection

**Nadya Rakovitsky,[1] Jonathan Lellouche,[1] Debby Ben David,[1,2] Sammy Frenk,[1] Polet Elmalih,[1] Gabriel Weber,[3,4] Hadas Kon,[1] David Schwartz,[1] Liat Wolfhart,[1] Elizabeth Temkin,[1] and Yehuda Carmeli[1,2]**

[1]National Institute for Antibiotic Resistance and Infection Control, Ministry of Health, Tel-Aviv, Israel ,[2]Sackler Faculty of Medicine, Tel-Aviv University, Tel-Aviv, Israel, [3]The B. Rappaport Faculty of Medicine, Technion, Israel Institute of Technology, Haifa, Israel, and [4]Infectious Disease and Infection Control Unit, Carmel Medical Center, Haifa, Israel

***Background.*** *Acinetobacter baumannii* is a successful nosocomial pathogen, causing severe, life-threatening infections in hospitalized patients, including pneumonia and bloodstream infections. The spread of carbapenem-resistant *Acinetobacter baumannii* (CRAB) strains is a major health threat worldwide. The successful spread of CRAB is mostly due to its highly plastic genome. Although some virulence factors associated with CRAB have been uncovered, many mechanisms contributing to its success are not fully understood.

***Methods.*** Here we describe strains of CRAB that were isolated from fulminant cases in 2 hospitals in Israel. These isolates show a rare hypermucoid (HM) phenotype and were investigated using phenotypic assays, comparative genomics, and an in vivo *Galleria mellonella* model.

***Results.*** The 3 isolates belonged to the ST3 international clonal type and were closely related to each other, as shown by Fourier-transform infrared spectroscopy and phylogenetic analyses. These isolates possessed thickened capsules and a dense filamentous extracellular polysaccharides matrix as shown by transmission electron microscopy (TEM), and overexpressed the capsule polysaccharide synthesis pathway-related *wzc* gene.

***Conclusions.*** The HM isolates possessed a unique combination of virulence genes involved in iron metabolism, protein secretion, adherence, and membrane glycosylation. HM strains were more virulent than control strains in 2 *G. mellonella* infection models. In conclusion, our findings demonstrated several virulence factors, all present in 3 CRAB isolates with rare hypermucoid phenotypes.

**Keywords.** carbapenem-resistant *Acinetobacter baumannii*; capsule; K-locus; mucoid phenotype; virulence.

*Acinetobacter baumannii* is an opportunistic pathogen associated with nosocomial infections with increasing importance to public health [1]. Its genome plasticity allows it to develop high-level antimicrobial resistance and environmental persistence [2]. CRAB causes severe infections with high morbidity and mortality, particularly pneumonia and bacteremia in critically ill mechanically ventilated patients with multiple invasive devices [3].

There are few studies of the correlation between laboratory findings of CRAB virulence and clinical outcomes. Most studies of CRAB virulence using animal models do not characterize clinical isolates and present limited data about patients [4]. We previously described 14-day mortality following CRAB bacteremia [5]. In that study, only 10% of deaths occurred within 48 hours, suggesting that fulminant CRAB bacteremia are not often reported. An in vivo model identified high bacterial fitness in a subgroup of Pasteur sequence types ST2 and ST3 that caused infections with high case fatality in humans [6]. While ST2 is a well-described international clonal, ST3 is found mostly in Mediterranean countries [6–8].

There are a number of virulence factors in *A. baumannii*, some of which are well characterized. *A. baumannii* virulence mechanisms include surface adhesins, glycoconjugates, micronutrient acquisition systems, and protein secretion [9, 10]. Capsule formation is an important virulence factor in various pathogenic bacteria, such as *Streptococcus pneumoniae* [11], *Escherichia coli* [12], and *Staphylococcus aureus* [13], and it is especially well described as a virulence factor in *Klebsiella pneumoniae* [14, 15]. Capsule formation has not been thoroughly described as a virulence factor in *A. baumannii*. In gram-negative bacteria, capsular polysaccharide biosynthesis loci (KL or K locus) and LPS loci (OCL or OC locus) are genetic "hot spots" that undergo changes at a higher rate. In loci with functions in capsule formation and organization, several important genes can be found, such *wza*, *wzc*, *itrA*, *qhbC*, and *qhbD*. Recently it was shown that *wza* gene knockout decreased

Received 16 March 2021; editorial decision 7 July 2021; accepted 18 July 2021.

Correspondence: Nadya Rakovitsky, PhD, National Institute for Antibiotic Resistance and Infection Control, Ministry of Health, Tel Aviv 64239, Israel (nadyarak@tlvmc.gov.il).

**Open Forum Infectious Diseases®2021**


https://doi.org/10.1093/ofid/ofab386

virulence of *A. bamuannii* and affected capsular polysaccharide synthesis and capsule thickness [16]. Chin and colleagues [17] described an *A. baumannii* subpopulation extracted from patients' blood showing a thicker capsule with abilities to switch phenotypic traits that control virulence.

In early 2019, 3 cases of fulminant CRAB bloodstream infection (BSI) in patients from 2 post–acute care hospitals (PACHs) were reported to the Israeli National Center for Infection Control. The high incidence of CRAB BSI compared with background incidence in this setting and the fulminant course in previously stable patients raised suspicions that an unusually virulent strain was involved, prompting this investigation. Here, we describe the 3 highly virulent strains of CRAB with a unique mucoid phenotype. We characterized the phenotype, evaluated in vivo virulence, and analyzed genomic content to identify factors that may have contributed to virulence.

## METHODS

A more detailed description of methods is available in the Supplementary Data.

### Bacterial Strains

Six *A. baumannii* isolates (5 CRAB strains and an American Type Culture Collection [ATCC] strain) were included in this study: the 3 BSI isolates (Ab905 [ST3], Ab238 [ST3], and Ab241 [ST3], hereafter referred to as "case isolates") and 3 controls. The controls were ATCC 19606 and 2 BSI isolates representing the most common sequence types in Israel (chosen randomly from the laboratory collections), ST2 (Ab105) and ST3 (Ab032) [6].

### Typing

Typing was performed by 2 methods: (1) the Pasteur scheme and (2) Fourier-transform infrared spectroscopy (FTIR; IR Biotyper, Bruker Daltonics, Bremen, Germany). Samples were prepared according to the IR Biotyper manufacturer's instructions. The specimens were analyzed in 4 replicates in 3 independent experiments. Spectra were analyzed using OPUS 7.5 software (Bruker Daltonics, Bremen, Germany). Quality control was performed according to the manufacturer's recommendations. A spectrum that failed to meet the quality control criteria was excluded from analysis. Hierarchical cluster analysis (HCA) was generated by OPUS 7.5 using the Pearson correlation coefficient option.

### Phenotypic Determination and Characteristics

Isolates were categorized by visual inspection as mucoid or nonmucoid [18]. The phenotype was also evaluated according to several colony morphology parameters, including texture, elevation, margin, size, and shape [19].

The motility assay was performed on semisolid Mueller-Hinton (MH) agar plates (MH + 0.25% agar W/W) and based on a protocol described previously for *A. baumannii* [20]. Plates were used on the same day they were prepared. Overnight culture was diluted (1:1000, ~$10^5$ colony-forming units [CFU]) in fresh MH and grown to an early logarithmic phase for 5 hours ($OD_{600}$ ~ 0.3, ~$1.5\times10^5$ CFU/mL). One microliter was inoculated by stabbing the agar in the center of the Petri dish and incubated for 18 ± 2 hours. Surface motility was evaluated by the pattern of branching, number of offshoot branches, and expansion distance between the inoculation point and the tentacle extremities. Four different experiments and 4 replicates in each experiment were performed for each isolate. We used a motile *A. baumannii* AB077 from our isolate collection and nonmotile ATCC 19606 as control strains.

Static biofilm biomass was determined using a semiquantitative microtiter plate assay. Overnight culture was diluted (1:1000) in fresh MH, grown to an early logarithmic phase, and normalized to a bacterial concentration of $OD_{600}$ 0.1 (~$5\times10^7$ CFU/mL). Aliquots of 200 µL were transferred to a sterile 96-well polystyrene microtiter plate (Nunc MicroWell 96-Well Microplates, Thermo Scientific) and incubated for 24 hours. Supernatants were removed by pipetting, and wells were washed 3 times with sterile phosphate-buffered saline (PBS) to remove planktonic cells. The biofilm biomass was dried by air for 30 minutes and stained with 0.1% crystal violet (Merck, Rehovot, Israel) solution for 15 minutes. The dye was removed by pipetting, and wells were washed 4 times with deionized water to remove the stain excess. The biofilm-associated dye was solubilized by adding 200 µL of 95% ethanol (molecular grade, 95%, BioLaB, Jerusalem, Israel). The biofilm biomass was quantified by measuring $OD_{540}$. Each isolate was tested in triplicate. Means and standard deviations were calculated. The statistical significance of the difference between the mucoid group and the control groups was determined using the Mann-Whitney *U* test.

The presence of capsule was confirmed using a density-dependent gradient test [18]. Results were read by visual observation: A bacterial band that migrated to the bottom phase of the gradient was classified as a noncapsulated strain, while a bacterial band that concentrated in the top phase was suspected to be a capsulated strain.

The capsule and the extracellular polysaccharides matrix were also imaged by transmission electron microscopy (TEM). The samples were prepared according to a standard protocol [21]. One milliliter of an overnight culture was centrifuged and fixed for 3 hours in Karnovsky fixative. Fixative residues were removed by washing with 0.1 M of sodium cacodylate buffer. The cells were post-fixed in 1% OsO4, 0.5% $K_2Cr_2O_7$, 0.5% $K_4[Fe(CN)_6]$ in 0.1 M of cacodylate-buffer (pH 7.4) for 1 hour at room temperature, then washed twice with 0.1 M of cacodylate-buffer and deionized water. Bacteria cells were stained with 2% uranyl-acetate for 1 hour and embedded in resin (Epon EMBED 812, EMS, Hatfield, PA, USA). The resin was polymerized at 60°C for 24 hours, and ultrathin sections (90–70 nm) were obtained using an ultramicrotome (UC7, Leica ultracat, Leica Biosystems; Buffalo Grove, IL,

USA). Samples were imaged at 120 kV (Tecnai G-12 Spirit, FEI, Hillsboro, OR, USA). Capsule thicknesses were obtained by measuring 15 different cells. Averages and standard deviations were calculated.

#### Quantification of *wzc* Expression

Three milliliters of an overnight culture was centrifuged, and total RNA was extracted using an automated benchtop system (MagNA Pure Compact RNA Isolation Kit with a MagNA Pure Compact Instrument, Roche Molecular Systems, Pleasanton, CA, USA) according the manufacturer's instructions. cDNA was obtained from 1 µg of total RNA using a reverse transcription kit (TaKaRa, Mountain View, CA, USA). Detection of *wzc* was performed using a primers set (fwd: CACCCAGCAATGCGTGAAAT; rev: GGTTCAACTGGCTCAACTGC) described previously for *A. baumannii* [16]. The quantification of *wzc* was calculated as the ratio of the expression level of *wzc* to the housekeeping gene *rpoB* and presented as the $\log_{10}$-fold change relative to ATCC 19606. The difference in *wzc* expression between the mucoid group and the control group was tested using a Mann-Whitney *U* test.

#### In Vivo Models

Two models of infection in *Galleria mellonella* were used: (1) killing assay [22] and (2) bacterial burden [22].

*G. mellonella* in the final-instar larval stage (TruLarv research grade, Biosystems, Devon, UK) were stored in the dark and used within 7 days of shipment. Caterpillars that were 250–350 mg in weight were used in all assays. Twelve randomly chosen caterpillars were used for each isolate. Each larva was injected with $10^5$ CFU in an inoculum of 20 µL using a syringe with a 32-G needle (Hamilton, Reno, NV, USA). Infected larvae were incubated at 32°C±5°C for 7 days in a dark environment, and the viability of the larvae was evaluated every 24 hours. Caterpillars were considered dead when they displayed no movement in response to touch and/or a change in color.

Bacterial fitness was determined 4 hours postinjection. To determine bacterial loads, larvae were homogenized individually in 1 mL of saline solution. Serial dilutions were plated on blood agar at 35°C±2°C for 24 hours. Results were presented as number of CFU per larvae. Nonmanipulated caterpillars (n = 4) and PBS-injected caterpillars (n = 4) were added as control groups. Each strain was tested in 2 experiments.

The survival curves of each group were compared using Kaplan-Meier curves, and the survival rates of the test group and each control group were compared using the log-rank test.

#### *DNA Extraction and Sequencing, Bioinformatics Analysis, and Phylogenetic Analysis*

A sequencing approach using short and long reads was used to obtain complete and closed genomes. Detailed description can be found in the Supplementary Data.

#### *K-loci Genetic Variability Determination*

K-loci and the lipooligosaccharide outer core (OCL) regions were identified using published annotations [23, 24].

#### *Data Availability*

All genomes were submitted to the NCBI genomics repository under BioProject number PRJNA605589. Accession numbers of the genomes can also be found in the NCBI repository under the accession numbers SAMN14072390 (Ab905), SAMN14072388 (Ab238), SAMN14072389 (Ab241), SAMN14072391 (Ab105), and SAMN14072392 (Ab032).

## RESULTS

#### Description of Cases

During a period of 4 months in 2018, 3 patients linked to a chronic ventilation ward in a post–acute care facility developed overwhelming sepsis. Three isolates (Ab241, Ab238, and Ab905) were sent to the National Institute for Antibiotic Resistance for further investigation.

Case No. 1: A 75-year-old woman underwent elective mitral valve replacement at Hospital A, with prolonged postoperative mechanical ventilation. After 2 months, she was transferred to the chronic mechanical ventilation ward of a PACH for rehabilitation. After an initial stable period, on day 10 she developed severe sepsis and was transferred to a tertiary care center. Blood cultures yielded CRAB, which was treated with meropenem and colistin. The patient recovered after prolonged antibiotic treatment.

Case No. 2: An 85-year old man was admitted to Hospital A with bacterial pneumonia, from which he recovered, but he remained ventilator dependent. After 2 months, he was transferred to the same PACH. After an initial stable period, he developed severe sepsis. He was treated with meropenem and colistin but died within 24 hours. Blood cultures grew CRAB.

Case No. 3: A 75-year-old man underwent a coronary arterial bypass in Hospital B and developed bilateral pneumonia. He recovered but remained ventilator dependent. He was transferred to the same PACH for rehabilitation. Eight days later, he developed a purulent sternal wound infection and was transferred to Hospital B. Debridement of the wound was performed on the same day. *Pseudomonas aeruginosa* was isolated from the wound and blood cultures. The patient improved after debridement. Four days later, he developed sepsis and multiple organ failure and died within a few hours. Blood cultures grew CRAB.

#### Relatedness of the Isolates

The 3 case isolates were classified as ST3 type by the Pasteur scheme. FTIR typing revealed that the 3 case isolates were very closely related and formed a distinct cluster compared with a convenience sample of other ST3 (n = 7) and ST2 (n = 8) isolates from our collection (Figure 1A).

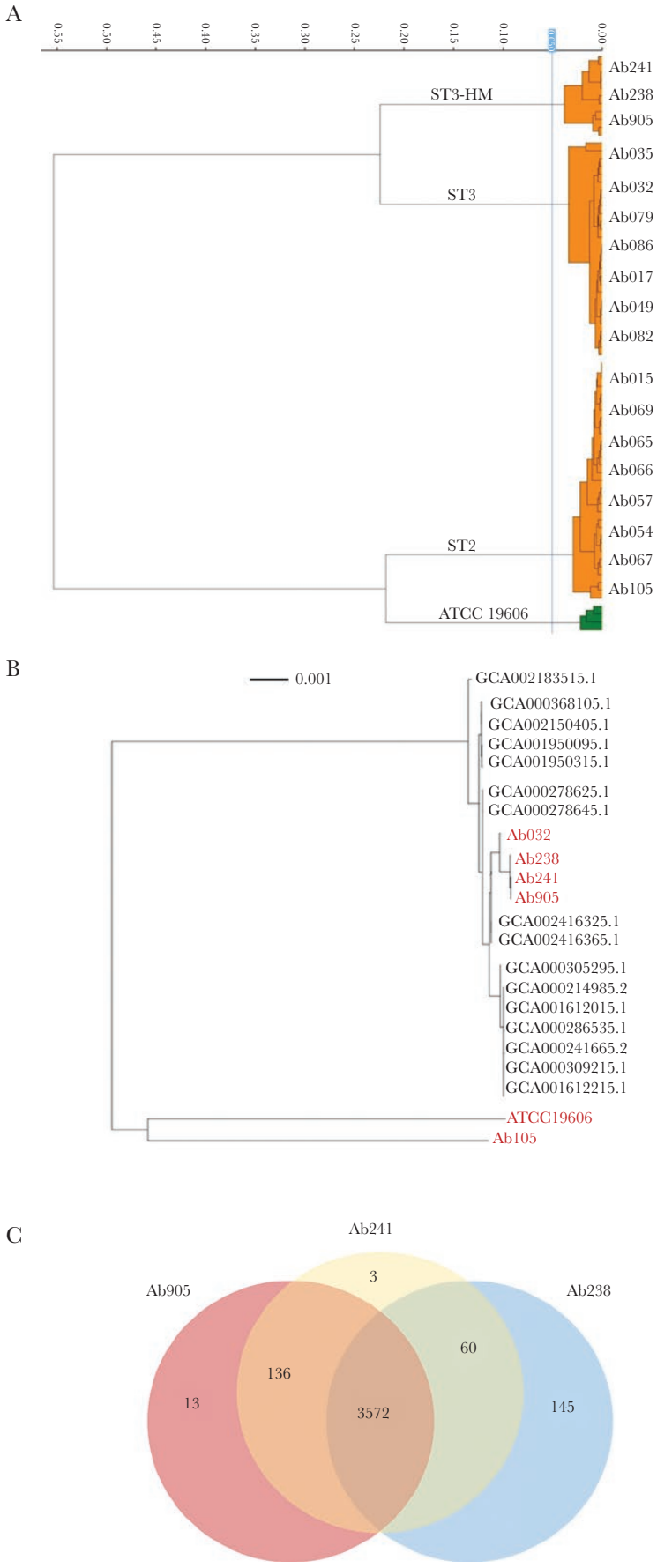
A
0.55
0.50
0.45
0.40
0.35
0.30
0.25
0.20
0.15
0.10
0.00
Ab241
Ab238
Ab905
ST3-HM
Ab035
Ab032
ST3
Ab079
Ab086
Ab017
Ab049
Ab082
Ab015
Ab069
Ab065
Ab066
Ab057
Ab054
ST2
Ab067
Ab105
ATCC 19606
B
0.001
GCA002183515.1
GCA000368105.1
GCA002150405.1
GCA001950095.1
GCA001950315.1
GCA000278625.1
GCA000278645.1
Ab032
Ab238
Ab241
Ab905
GCA002416325.1
GCA002416365.1
GCA000305295.1
GCA000214985.2
GCA001612015.1
GCA000286535.1
GCA000241665.2
GCA000309215.1
GCA001612215.1
ATCC19606
Ab105
C
Ab241
Ab905
Ab238
3
60
136
13
3572
145

Core genome alignment of the case isolates showed that they were closely grouped in a unique branch of the phylogenetic tree when compared with the 16 available ST3 genomes from public databases and with Ab032, an ST3 from our collection (Figure 1B).

For further testing, we chose 2 comparator CRAB isolates from our collection: Ab032 (ST3) and Ab105 (ST2), and an ATCC strain (ATCC 19606). According to the pangenome, there were 3572 shared core genes (Figure 1C), on which phylogenetic analysis was based. There were 13 unique genes found in Ab905, 3 unique genes in Ab241, and 145 unique genes in Ab238.

#### Antibiotic Resistance

The case isolates were extremely drug-resistant (XDR). They were resistant to meropenem (minimum inhibitory concentration [MIC] ≥16 mg/L), ampicillin/sulbactam (MIC 16mg/L), ceftazidime (MIC ≥64 mg/L), ciprofloxacin (MIC ≥4 mg/L), and had an elevated MIC of 8 mg/L to gentamicin. They were susceptible to colistin (MIC 0.5 mg/L) and tigecycline (MIC 1 mg/L).

Genomic analysis showed that the case isolates harbored multiple antibiotic resistance genes. They shared the genes encoding the aminoglycoside-modifying enzymes O-nucleotidyl transferases *ant(2')-Ia* and *ant(3')-IIa*, a $bla_{OXA-23}$ carbapenemase, a $bla_{ADC-6}$ *ampC* cephalosporinase, *tet(A)* efflux MFS transporter, and *gyrA/parC* DNA gyrase and topoisomerase IV, respectively. The case isolates expressed the intrinsic $bla_{OXA-51}$ gene. However, the *ISabA1* insertion system was not found upstream.

Several resistance genes differed between the case isolates. The *aph(3')-VIa* gene encoding the aminoglycoside-modifying enzyme O-phosphotransferase was present in Ab238 and Ab241, but not in Ab905. The *aac(3)-I* gene encoding the aminoglycoside-modifying enzyme N-acetyltransferase was present only in Ab238. The genes *qacE* and *sul1* encoding the quaternary ammonium compound resistance protein and the dihydropteroate synthase, respectively, were present only in Ab905. The control strains Ab105 and Ab032 had different resistomes (Supplementary Table 1).

#### Hypermucoid Phenotype

The 3 case isolates showed an unusual hypermucoid phenotype. HM–*A. baumannii* appeared on agar plates as a slime layer, and colonies were opaque, moist, and raised with irregular margins, while the nonmucoid control strains (Ab105, ATCC 19606) displayed a typical phenotype of small, round colonies with distinct margins (Figure 2). The ST3 control strain, Ab032, and the 3 case strains appeared more mucoid than non-ST3 strains. All isolates tested negative by string test. After multiple transfers on blood agar plates and on chocolate agar, the HM phenotype persisted. When isolates were grown on other media, such as MacConkey and Muller Hinton (MH), the HM phenotype was not consistently apparent, but when transferred back to blood or chocolate agar the HM phenotype became evident again. The addition of 5% $CO_2$ to the environment during incubation increased the HM phenotype of the isolates.

In the density gradient assay, the 3 case strains and the ST3 control strain Ab032 migrated only to the top phase, indicating capsulated bacteria. The control strains Ab105 and ATCC 19606 migrated to the bottom phase, indicating the lack of a capsule (Figure 3A). Likewise, TEM imaging revealed that the 3 case isolates and the ST3 control strain Ab032 were capsulated (Figure 3B). Capsule thickness ranged from 84 ± 18 nm to 115 ± 16 nm (Figure 3C). In contrast, no capsule was found in the Ab105 and ATCC 19606 strains. India ink staining produced similar results (Supplementary Figure 1). In addition, TEM imaging showed a dense filamentous extracellular polysaccharides (EPS) matrix in study strains.

#### Motility of the HM Strains

Surface-associated motility analysis show that all case strains and the control ST3 strain Ab032 were highly motile, extending multiple growth arms, while the non-ST3 strains were slightly motile (Ab105) or nonmotile (ATCC 19606) (Figure 5). The motility was measured by branch length and statistical analysis, represented in Supplementary Figure 2.

#### Virulence Determinants

Complete genomes of 3 strains (Ab241, Ab238, and Ab105) and draft genomes of 2 strains (Ab905 and Ab032) were obtained. Comparison of genomes to the Virulence Factor Database (VFDB) found that all 3 case isolates possessed 36 virulence genes. The virulence functions of these genes were as follows: 3 belonged to the phospholipase C and D enzyme clusters, 17 were involved in iron uptake (acinetobactin), 13 were involved in biofilm formation (csu fimbriae, PNAG, AdeFGH efflux pump), 1 was involved in adherence (OmpA), and 2 were involved in capsule regulation (BfmrS) (Supplementary Table 2).

**Figure 1.** Phenotypic and genomic relationship of *A. baumannii* strains. A, Phenotypic relationship between the case CRAB isolates (Ab238, Ab241, Ab905) and controls, as determined by FTIR spectroscopy analysis. Controls consisted of control strain ATCC 19606 (OXA-98, ST52 by Pasteur), classified as an unrelated singleton, 8 CRAB ST2 isolates (Ab015, Ab069, Ab065, Ab066, Ab057, Ab054, Ab067, Ab105), and 7 CRAB ST3 isolates (Ab035, Ab032, Ab079, Ab086, Ab017, Ab049, Ab082) from our collection. B, Core genome alignment of the 4 ST3 study isolates (in red) compared with 20 ST3 genomes available from public databases. Ab105 (ST2) and *A. baumannii* ATCC 19606 (ST52; in red) were added as representative strains with unrelated ST types. The study ST3 strains were most similar to ST3 strains from 2 patients with pneumonia in the United States (OIFC137 and OIFC109; Washington DC, USA) and 2 strains isolated from skin swabs in Switzerland (AC003 and AC003-2-R1; Geneva, Switzerland). C, Venn diagram of co-occurring and unique genes found in the 3 case isolates' genomes relative to the ST3 control strain Ab032 and the database-derived genomes. Overlapping regions indicate genes shared by 2 or 3 case strains. Nonoverlapping regions indicate genes present in 1 case strain and absent in Ab032 and all database genomes. Abbreviations: ATCC, American Type Culture Collection; CRAB, carbapenem-resistant *Acinetobacter baumannii*; FTIR, Fourier-transform infrared spectroscopy.

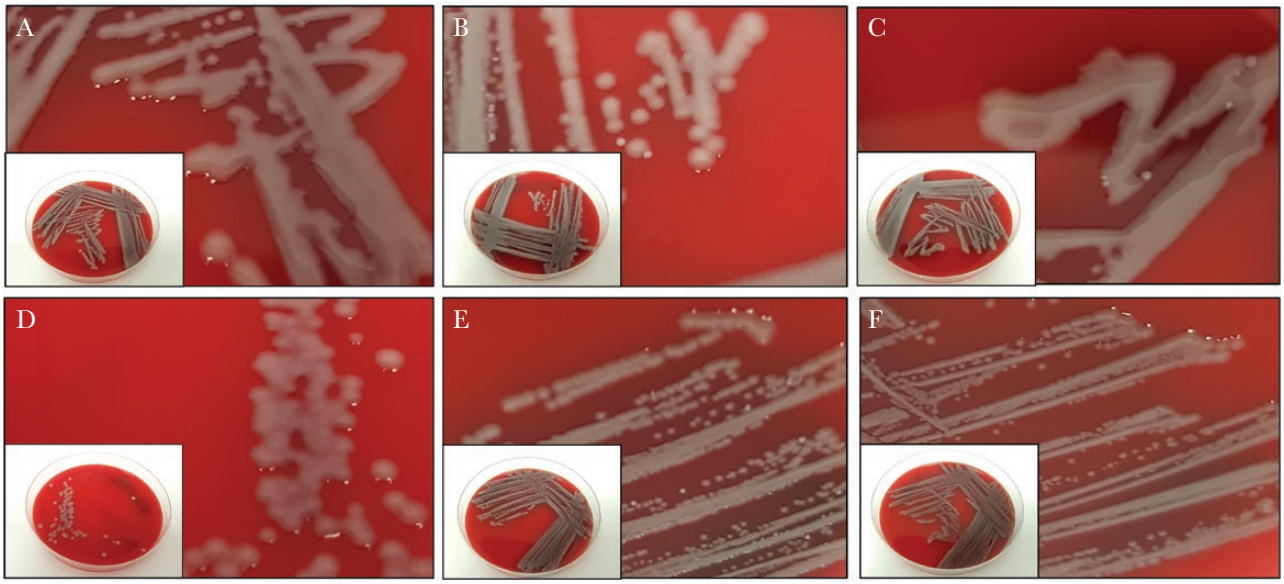


**Figure 2.** Colony phenotype of hypermucoid ST3 strains. Hypermucoid phenotype of the 3 specimens isolated from patients with fulminant bacteremia: (A) Ab905, (B) Ab238, and (C) Ab241. D, ST2-Ab032 and (E) ST3-Ab105 were added as isolates representing the most common clonal lineages in Israel. F, *A. baumannii* ATCC 19606 was included as a control. Phenotype was determined following 18 ± 2 hours of incubation at 35°C±2°C on blood agar. Abbreviation: ATCC, American Type Culture Collection.

The case isolates Ab241 and Ab905, but not Ab238, also possessed the quorum-sensing loci *abaI* and *abaR*. As for the control strains Ab032 and Ab105, they possessed 3 phospolipase C and D enzyme clusters; 19 and 18, respectively, were involved in iron uptake (acinetobactin); 14 and 13, respectively, were involved in biofilm formation, and both possessed the quorum-sensing genes *abaI* and *abaR*.

Analysis of the K locus of the case isolates and the ST3 control strain showed the presence of KL17. We compared the KL17 locus of the case isolates to that of *A. baumannii* isolate G7 (GCA_000214985.2), in which KL17 was originally described. The KL17 locus of the case isolates did not include any insertion sequence or a recombination event, but differed from *A. baumannii* isolate G7 by 30 insertion/deletion mutations and 320 mismatch mutations. The distribution of these mutations was uneven on the locus and was more frequent in the *itrA*, *qhbC*, and *qhbB* genes and less frequent in *wzc* and *wza* (Figure 4A). High diversity was also found in *qhbC* and *qhbB*, the genes responsible for the synthesis of UDP-D-QuipNAc4NR, and *itrA*, a gene coding for an initiating transferase (Figure 4A). Analysis of the expression levels of the *wzc* gene, which regulates the export of capsular polysaccharide, showed significantly decreased levels in the Ab105 isolate and significantly increased levels ($P < .05$) in all capsulated isolates (Ab238, Ab905, Ab241, and Ab032) in comparison to control strain ATCC19606 (Figure 4B).

We assembled circular chromosomes and plasmids for study strains. All 3 case strains carried a 8507-bp-long plasmid coding for a unique replication initiation gene, a toxin antitoxin addiction mechanism, a *tonB*-dependent outer membrane receptor gene, a gene encoding a cholesterol-dependent cytolysin (septicolysin), and other hypothetical proteins (Supplementary Table 3). The plasmid did not carry any antibiotic resistance genes, and $bla_{oxa\text{-}23}$ was found on the chromosome. We named the plasmid pTLV-1. pTLV-1 is highly similar to the previously described *A. baumannii* plasmids CP010782 (plasmid pA1-1) and KX230793.1.

Case isolates Ab905 and Ab241 carried no additional plasmids. Case isolate Ab238 carried both pTLV-1 (7 times more copies than the chromosome) and a 70 544-bp-long RepAci6 plasmid with Tra operon, which suggests that it can transfer by conjugation (1.7 times more copies than the chromosome). Isolate Ab105, the ST2 control strain, had 2 mobile genetic elements. The first was a 10 879-bp-long plasmid with a RepAci1 replicon gene (13 more copies than the chromosome), which carried a septicolysin gene (similar to the ST3 study isolates) and 2 $bla_{OXA\text{-}24}$ genes. The second was a 1 110 967-bp-long genetic mobile element that had many phage genes and hypothetical proteins.

#### Biofilm and In Vivo Virulence Models

As biofilm formation is known to contribute to bacterial virulence [9], we next decided to examine this phenotype. The case strains and the ST3 control strain Ab032 had greater biofilm formation on polystyrene microtiter plates, compared with the control ST2 strain (Ab105) and ATCC 19606 (Figure 6A). Planktonic growth did not differ between the 6 strains (data not shown).

To assess virulence in vivo, we used 2 models in the *Galleria mellonella* waxworm: a survival model and a fitness model. In the 24-hour survival model, injection of $10^5$ CFU per larva into the case isolates led to variable mortality rates (54.2%–97.9%),

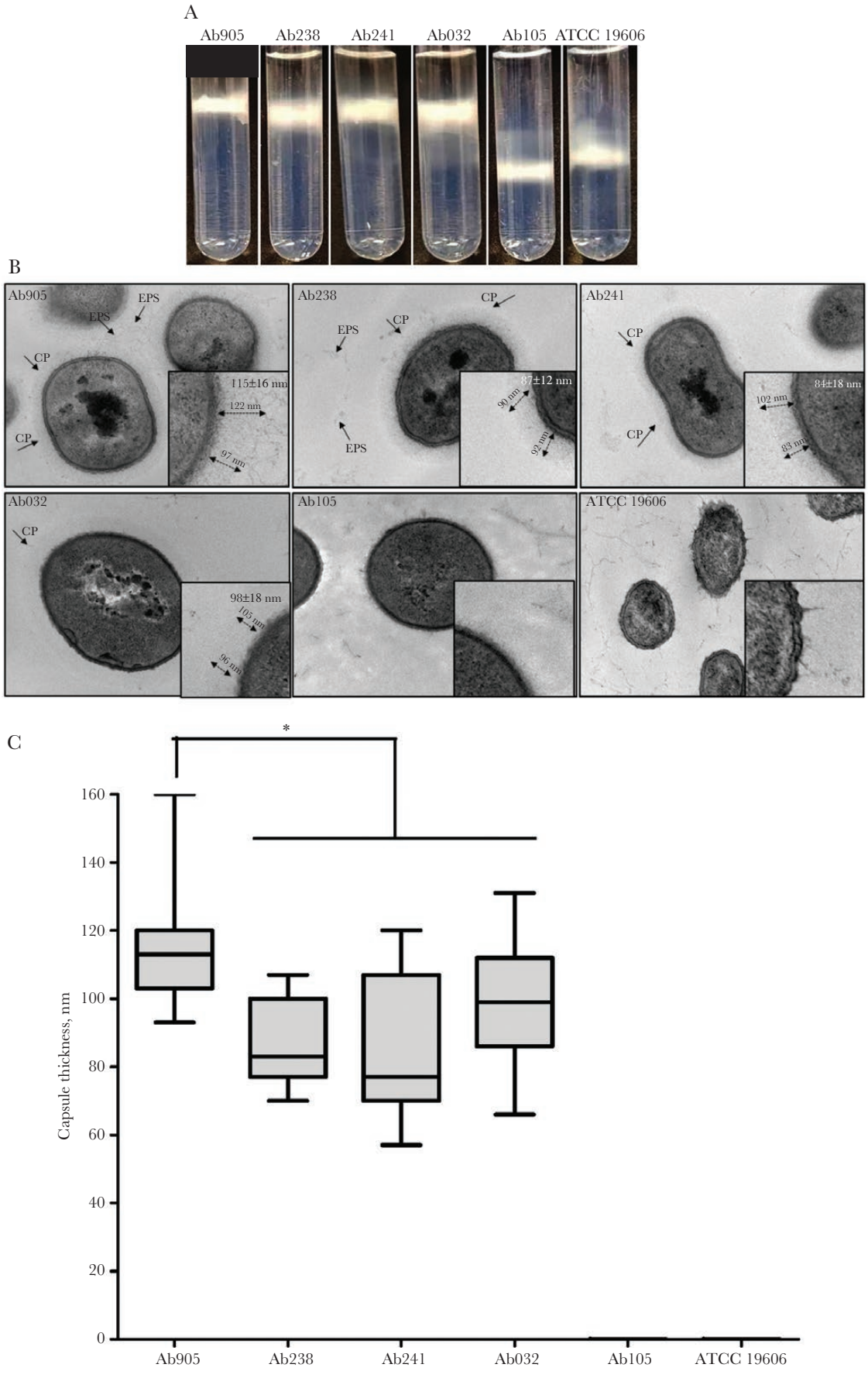
A
Ab905
Ab238
Ab241
Ab032
Ab105
ATCC 19606
B
Ab905
EPS
EPS
CP
CP
115±16 nm
122 nm
97 nm
Ab238
CP
EPS
CP
EPS
87±12 nm
90 nm
92 nm
Ab241
CP
CP
84±18 nm
102 nm
83 nm
Ab032
CP
98±18 nm
105 nm
96 nm
Ab105
ATCC 19606
C
*
Capsule thickness, nm
160
140
120
100
80
60
40
20
0
Ab905
Ab238
Ab241
Ab032
Ab105
ATCC 19606

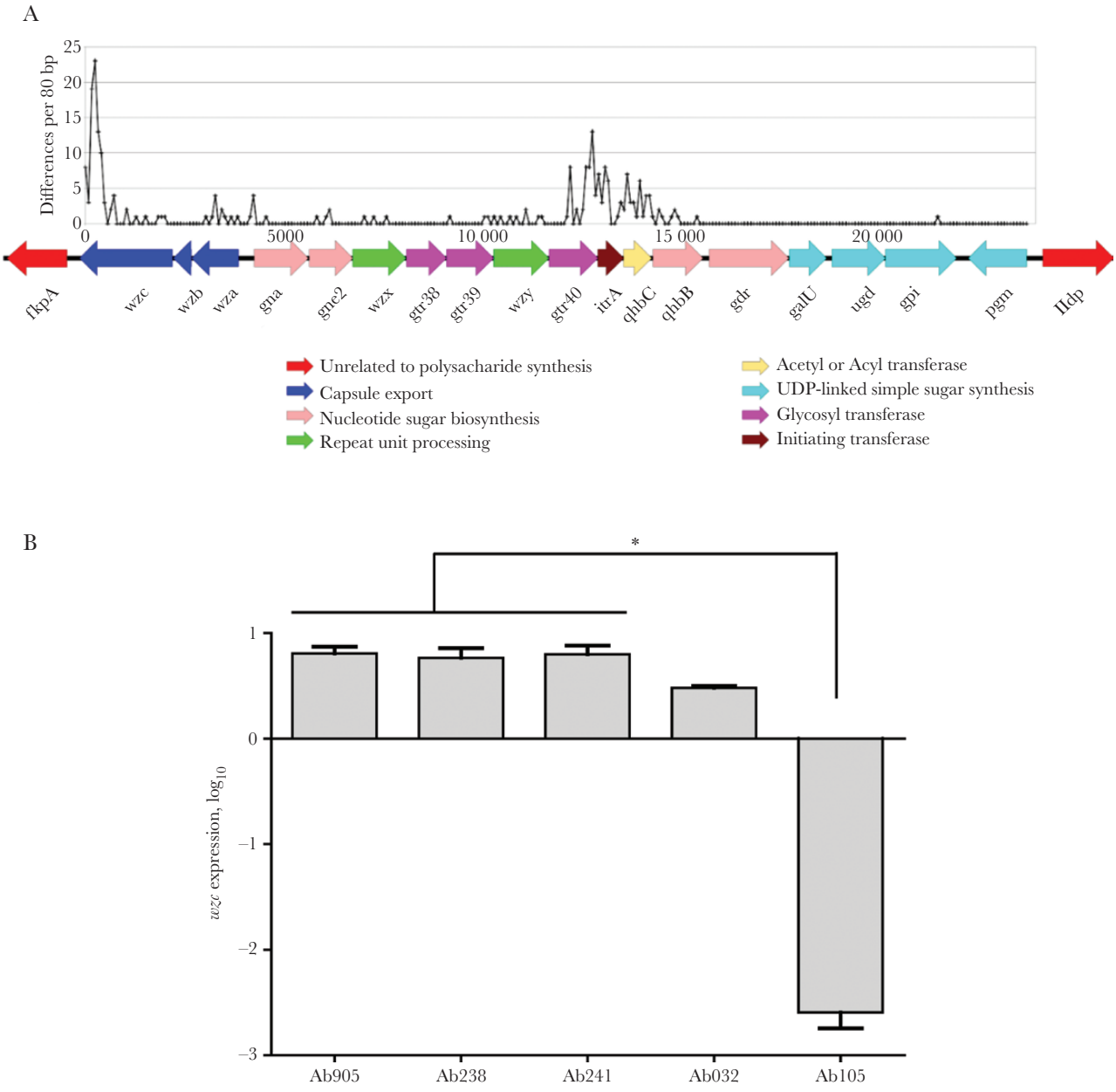


**Figure 4.** KL locus structure and expression. (A) KL17 structure and genetic variation on HM-ST3 isolates. Variation was calculated as the mean number of SNPs per 80-bp in the HM-ST3 isolates compared with a KL17 control strain (GCA_000214985.2). (B) Relative expression of the wzc gene was normalized to the basal level of wzc expression measured in ATCC 19606 following 18 ± 2 hours of incubation at 35°C ± 2°C. Mean and SDs were calculated from 4 replicates. *Mann-Whitney U test was performed; $P <$ .05 for comparison of each of the ST3 strains to AB105. Abbreviations: ATCC, American Type Culture Collection; SNP, single nucleotide polymorphism.

which were much higher than the ATCC 19606 mortality rate (4.2%; $P < .001$) but did not differ between the case isolates and the clinical control isolates (Figure 6B).

In the bacterial fitness model, 4 hours after injection of $10^5$ CFU per larva, the average bacterial count increased for all larvae injected with case isolates: an increase of 2.6 $\log_{10}$ CFU for Ab238, 1.5 $\log_{10}$ CFU for Ab905, and 1.9 $\log_{10}$ CFU for Ab241. In contrast, the average bacterial count decreased in the control strains, by 0.2 times in Ab105 and by 1.2 times in ATCC 19606 (Figure 6C). After in vivo growth in *Galleria melonella*,

**Figure 3.** Capsule characterization of the HM-ST3 strains. A, Capsule presence confirmation in the HM-ST3 isolates by a density-dependent gradient assay. B, Representative TEM images of the HM-ST3 isolates (Ab238, Ab241, Ab905), Ab105 (ST2), Ab032 (ST3), and ATCC 19606 following 18 ± 2 hours of incubation at 35°C±2°C on blood agar. Black arrows indicate CP and filamentous EPS. Inserts show enlargement of the bacterial cell wall and the associated capsule. The numbers in the inserts are the mean and standard deviation of the capsule thickness measured in 5 places in 3 cells. Abbreviations: ATCC, American Type Culture Collection; CP, bacterial capsule; EPS, extracellular polysaccharides; HM, hypermucoid; SNP, single nucleotide polymorphism..

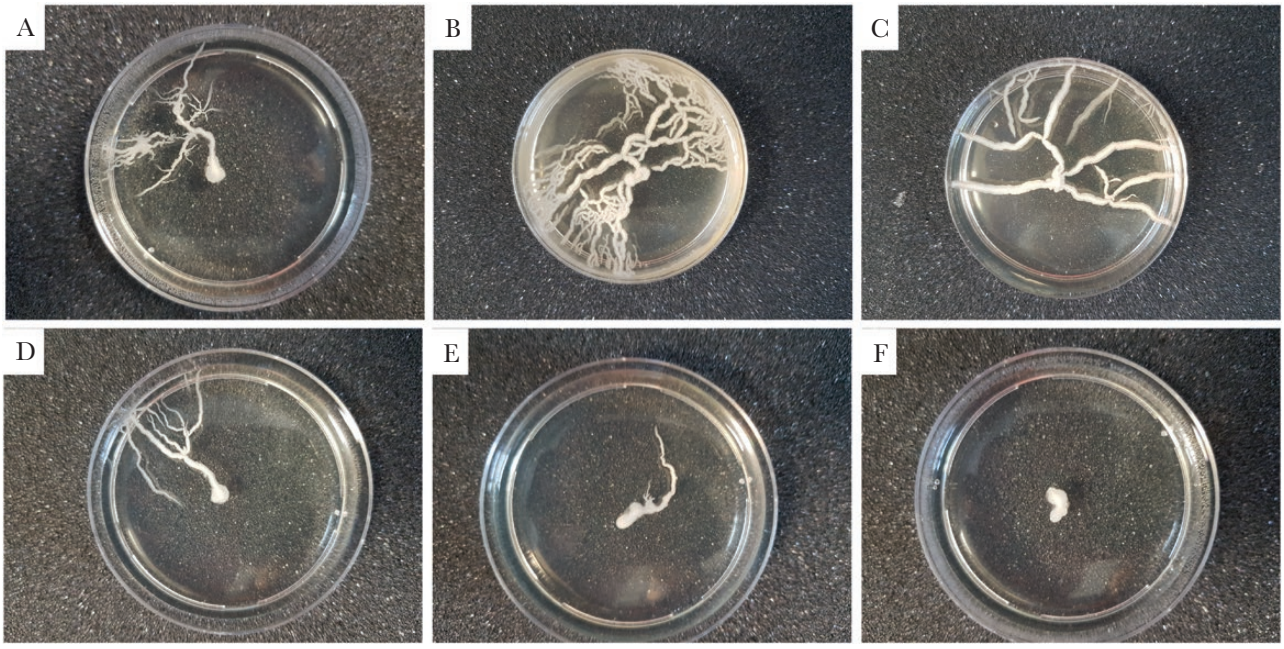


**Figure 5.** Phenotypic characterization of study isolates. Motility of case and control isolates on MH semisolid agar. Motility patterns of the 3 case isolates: (A) Ab238, (B) Ab241, and (C) Ab905; and 3 control isolates: (D) Ab032 (ST2), (E) Ab105 (ST3), and (F) ATCC 19606. Plates were visualized following 18 ± 2 hours of incubation at 35°C±2°C. Abbreviations: ATCC, American Type Culture Collection; MH, Mueller-Hinton.

all 4 ST3 strains formed mucoid phenotype colonies on blood agar plates, whereas ST2 and ATCC 19606 did not.

## DISCUSSION

*Acinetobacter baumannii* is an opportunistic bacterium and a well-known cause of nosocomial infections. While the virulence of *A. baumannii* has been questioned [25], this pathogen is increasingly reported to be involved in extremely fulminant infections [26]. Over the last decade, large studies have reported high case fatality rates among patients with bacteremia and pneumonia caused by CRAB [5, 26, 27]. Here, we investigated a cluster of CRAB bacteremia cases exhibiting an unusual fulminant course in previously stable patients. We found that the 3 cases were caused by a single clone of CRAB closely grouped in a unique branch of the phylogenetic tree ST3 harboring an unusual hypermucoid phenotype. In a single-center study in Israel conducted in 2008–2011, ST3 was responsible for 16.9% of the CRAB bacteremia cases [5]. We also found that the 3 case strains were closely related by FTIR analysis, suggesting close similarity in the carbohydrates, and formed a distinct cluster when compared with other ST3 strains.

Few studies have examined the virulence of ST3, with conflicting results. De Breij et al. reported that ST3 strains showed lower virulence than ST1 and ST2 strains in an experimental pneumonia model [28]. In contrast, Nutman et al. found that 14-day mortality in patients with bacteremia caused by ST3 strains was remarkably high. These strains when examined in a mouse model also revealed increased fitness [6].

We found that the 3 case isolates were armed with multiple mechanisms of resistance responsible for the XDR phenotype. We were able to show the presence of a spectrum of virulence genes in all outbreak isolates, including the phospholipase C/D family, acinetobactin family, ompA, BfmrS, and others. Several phenotypic characteristics associated with virulence were apparent. The first was an unusual hypermucoid phenotype that was clearly and consistently apparent on blood and chocolate agar and was maintained after growth in the *Galleria melonella* host. A hypermucoid phenotype is a recognized virulence factor in various bacteria [29–31]. A hypermucoid phenotype usually represents overproduction of mucopolysacharides, leading to a thick capsule that protects the bacteria from opsonization and the host immune response and disturbs the entry of antimicrobials into the cell [32]. Density gradient centrifugation suggested that the case isolates were capsulated. Indeed, TEM imaging revealed a thick capsule and a dense filamentous EPS matrix. We demonstrated the overexpression of the *wzc* gene, which likely contributed to the hypermucoid phenotype and may be related to the K-locus modifications.

The second virulence characteristic was motility. While the name *Acinetobacter* was given to the species to denote its nonmotility (from the Greek *akineto*), some strains show motility in semisolid media [33]. Hua et al. [34] showed that strains with polysaccharide overexpression are more motile, and other studies showed that motility in CRAB correlates with virulence

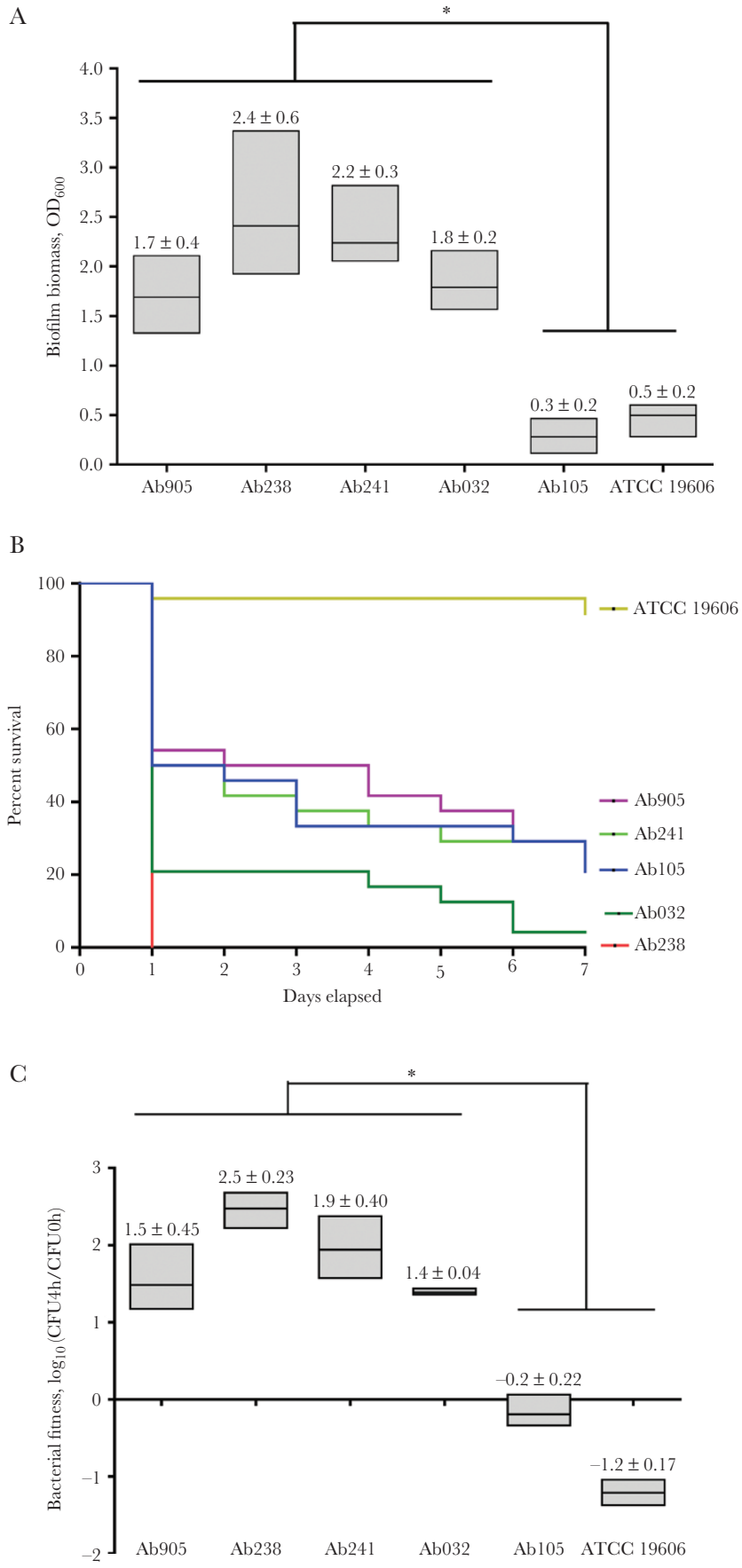
A
*
Biofilm biomass, OD600
4.0
3.5
3.0
2.5
2.0
1.5
1.0
0.5
0.0
1.7 ± 0.4
2.4 ± 0.6
2.2 ± 0.3
1.8 ± 0.2
0.3 ± 0.2
0.5 ± 0.2
Ab905
Ab238
Ab241
Ab032
Ab105
ATCC 19606
B
Percent survival
100
80
60
40
20
0
0
1
2
3
4
5
6
7
Days elapsed
ATCC 19606
Ab905
Ab241
Ab105
Ab032
Ab238
C
*
Bacterial fitness, log10 (CFU4h/CFU0h)
3
2
1
0
−1
−2
1.5 ± 0.45
2.5 ± 0.23
1.9 ± 0.40
1.4 ± 0.04
−0.2 ± 0.22
−1.2 ± 0.17
Ab905
Ab238
Ab241
Ab032
Ab105
ATCC 19606

[35] Here, all ST3 case strains as well as the ST3 control strain were highly motile and extended multiple growth arms in semisolid media.

The third virulence characteristic found in our isolates was biofilm formation. Biofilm formation enables a bacterium to survive on surfaces in the medical environment [9], in exposure to environmental stress and disinfectants. In a previous report by Tipton et al. [36], a highly virulent subpopulation of *A. baumannii* with a thick capsule but reduced biofilm formation was described, suggesting that biofilm formation plays no role in the virulence of this bacterium. However, our case isolates were more biofilm-forming than the control isolates. These results suggest that, at least in some cases, biofilm formation by *A. baumannii* contributes to *A.baumannii* pathogenicity and promotes fulminant infection.

Our in vivo model of virulence showed lower survival of *G. mellonella* when the case isolates were compared with the ATCC strain, but no differences in survival when compared with the clinical control strains. On the other hand, when fitness was measured by 4-hour in vivo growth in *G. mellonella,* the case strains reached a higher bacterial load than both the ATCC and the clinical control strains. As virulence characteristics differ between hosts and model systems, this discrepancy highlights the need to carefully choose the appropriate in vivo model system to study bacterial virulence.

We identified a common plasmid in all 3 case isolates, pTLV-1, which encodes for *ton-B*, *septicolysin*, and *brnT/brnA* toxin–antitoxin systems. Ton-B is a copper receptor that plays a role in adherence to epithelial cells [37]. Septicolysin is a predicted pore-forming toxin [38], a potential virulence factor, which has been described in *Clostridium septicum*, *Bacillus anthracis*, and *Streptococcus pneumonia* [39], but its function has not been reported in *A. baumannii* so far. A plasmid similar to pTLV-1, named pA1-1, was recently found in an *A. baumannii* ST2 isolate from Australia [40]. Another similar plasmid, named pMAL-1, was isolated in Serbia (GenBank KX230793.1), in *A. baumannii* ST3. pMAL-1 carrying OXA-72 gene and ton-B gene, but not carrying *septicolysin* gene. In *K. pneumonia*, the hypermucoid phenotype has been described as a plasmid-acquired phenotype. For example, Gu et el. [41] reported acquisition of the pLVPK-like virulence plasmid, which encodes 2 capsular polysaccharide (CPS) regulator genes (rmpA and rmpA2) and several siderophore gene clusters in *K. pneumoniae* ST11. In contrast, the pTLV-1 plasmid did not include genes coding for a hypermucoid phenotype and did not carry any antibiotic resistance determinant; its role in conferring virulence remains to be determined.

Our study has limitations. First, although we identified several virulence characteristics and genes, we have not shown their direct effect. Particularly, we did not prove that the hypermucoid phenotype caused the increased virulence; we did not conduct experiments modifying the mucoid phenotype. However, as a hypermucoid phenotype is a recognized virulence factor, we believe that this is also the case here. Second, our in vivo models were conducted in a single host, *G. mellonella*. The effects of various virulence factors may differ between hosts. Taken together, our results highlight the importance of monitoring CRAB outbreaks for mucoid/nonmucoid phenotypes and of developing an identification method for mucoid CRAB.

## Supplementary Data

Supplementary materials are available at Open Forum Infectious Diseases online. Consisting of data provided by the authors to benefit the reader, the posted materials are not copyedited and are the sole responsibility of the authors, so questions or comments should be addressed to the corresponding author.


## Acknowledgments

We would like to thank all the staff at the National Institute for Antibiotic Resistance and Infection Control, Ministry of Health, Tel-Aviv Sourasky Medical Center.

***Author contributions.*** N.R. conceived and planned the experiments. S.F. designed and performed the bioinformatics work. P.E. and N.R. performed *G. mellonella* experiments. H.K. performed real-time PCR and gradient assay experiments with supervision from N.R. J.L. contributed to the interpretation of the results. L.W. did statistical analysis. N.R. wrote the manuscript in consultation with E.T., D.B.D., G.W., D.S., and Y.C. All authors discussed the results and commented on the manuscript.

***Patient consent.*** No human subjects were involved in this study.

***Financial support.*** This work was supported by the National Institute for Antibiotic Resistance and Infection Control, Ministry of Health, Israel as part of the unit's routine work.

***Potential conflicts of interest.*** All authors: no reported conflicts of interest. All authors have submitted the ICMJE Form for Disclosure of Potential Conflicts of Interest. Conflicts that the editors consider relevant to the content of the manuscript have been disclosed.


**Figure 6.** Biofilm formation. A, Determination of the biofilm biomass formed by HM-ST3 case isolates (Ab238, Ab241, Ab905) and controls (Ab105 [ST2], Ab032 [ST3], and ATCC 19606) using a microtiter static biofilm model. The biofilm biomass was quantified following 18 ± 2 hours of incubation at 35°C±2°C. Box plots depict the mean biomass (central horizontal lines) and minimal/maximal values (boxes). Numerical values are the mean and standard deviation. Each isolate was tested by 5 replicates in 2 different experiments. Stars represent the statistical significance of the difference between the HM-ST3 group and the Ab032 (*$P$ = .151(, Ab105 (**$P$ = .001(, and ATCC 19606 (***$P$ = .003) control strains. In vivo virulence of the HM-ST3 case strains. B, Survival of Galleria mellonella larvae infected with HM-ST3 case isolates (Ab238, Ab241, Ab905). Larvae were inoculated with 1.0×105 CFU and monitored for 7 days. Comparison between the HM-ST3 strains group and each control strain survival curve was carried out using the log-rank test: Ab238 vs ATCC 19606 ($P$ < .005), Ab238 vs Ab105 ($P$ < .005), Ab238 vs Ab032 ($P$ = .02); log-rank test for Ab905 and Ab241 vs ATCC 19606 ($P$ < .005), Ab905 and Ab241 vs Ab105 ($P$ = .565), Ab905 and Ab241 vs Ab032 ($P$ = .009). C, Bacterial fitness of the HM-ST3 case strains (Ab238, Ab241, Ab905) in Galleria mellonella larvae 4 hours postinoculation. Ab105 (ST2), Ab032 (ST3), and ATCC 19606 were added as control strains. Stars indicate the statistical significance of the difference between the HM-ST3 group (Ab905, Ab238, and Ab241) and the Ab032 (*$P$ = .195), Ab105 (**$P$ = .016), and ATCC 19606 (***$P$ = .016) control strains. Abbreviations: ATCC, American Type Culture Collection; CFU, colony-forming units; CP, bacterial capsule; EPS, extracellular polysaccharides; HM, hypermucoid; SNP, single nucleotide polymorphism.

## References


1. Voidazan S, Albu S, Toth R, Grigorescu B, Rachita A, Moldovan I. Healthcare associated infections—a new pathology in medical practice? Int J Environ Res Public Health. **2020**; 17:760.
2. Traglia G, Chiem K, Quinn B, et al. Genome sequence analysis of an extensively drug-resistant *Acinetobacter baumannii* indigo-pigmented strain depicts evidence of increase genome plasticity. Sci Rep **2018**; 8:16961.
3. Wong D, Nielsen TB, Bonomo RA, et al. Clinical and pathophysiological overview of *Acinetobacter* infections: a century of challenges. Clin Microbiol Rev **2017**; 30:409–47.
4. Hua M, Liu J, Du P, et al. The novel outer membrane protein from OprD/Occ family is associated with hypervirulence of carbapenem resistant *Acinetobacter baumannii* ST2/KL22. Virulence. **In press**.
5. Nutman A, Glick R, Temkin E, et al. A case-control study to identify predictors of 14-day mortality following carbapenem-resistant *Acinetobacter baumannii* bacteraemia. Clin Microbiol Infect **2014**; 20:O1028–34.
6. Nutman A, Lellouche J, Lifshitz Z, Glick R, Carmeli Y. In vivo fitness of *Acinetobacter baumannii* strains in murine infection is associated with international lineage ii-rep-2 and international lineage iii clones showing high case fatality rates in human infections. Microorganisms **2020**; 8:2–9.
7. Pournaras S, Gogou V, Giannouli M, et al. Single-locus-sequence-based typing of blaOXA-51-like genes for rapid assignment of *Acinetobacter baumannii* clinical isolates to international clonal lineages. J Clin Microbiol **2014**; 52:1653–7.
8. Karah N, Dwibedi CK, Sjöström K, et al. Novel aminoglycoside resistance transposons and transposon-derived circular forms detected in carbapenem-resistant *Acinetobacter baumannii* clinical isolates. Antimicrob Agents Chemother **2016**; 60:1801–18.
9. Harding CM, Hennon SW, Feldman MF. Uncovering the mechanisms of *Acinetobacter baumannii* virulence. Nat Rev Microbiol **2018**; 16:91–102.
10. Vijayakumar S, Rajenderan S, Laishram S, et al. Biofilm formation and motility depend on the nature of the *Acinetobacter baumannii* clinical isolates. Front Public Health **2016**; 4:105.
11. Paton JC, Trappetti C. *Streptococcus pneumoniae* capsular polysaccharide. Microbiol Spectr **2019**; 7.
12. Goller CC, Seed PC. Revisiting the *Escherichia coli* polysaccharide capsule as a virulence factor during urinary tract infection: contribution to intracellular biofilm development. Virulence **2010**; 1:333–7.
13. Rausch M, Deisinger JP, Ulm H, et al. Coordination of capsule assembly and cell wall biosynthesis in *Staphylococcus aureus*. Nat Commun **2019**; 10:1404.
14. Pan YJ, Lin TL, Chen CT, et al. Genetic analysis of capsular polysaccharide synthesis gene clusters in 79 capsular types of *Klebsiella* spp. Sci Rep **2015**; 5:15573.
15. Choby JE, Howard-Anderson J, Weiss DS. Hypervirulent *Klebsiella pneumoniae*—clinical and molecular perspectives. J Intern Med **2020**; 287:283–300.
16. Niu T, Guo L, Luo Q, et al. Wza gene knockout decreases *Acinetobacter baumannii* virulence and affects Wzy-dependent capsular polysaccharide synthesis. Virulence **2020**; 11:1–13.
17. Chin CY, Tipton KA, Farokhyfar M, Burd EM, Weiss DS, Rather PN. A high-frequency phenotypic switch links bacterial virulence and environmental survival in *Acinetobacter baumannii*. Physiol Behav **2017**; 176:139–48.
18. Kon H, Schwartz D, Temkin E, Carmeli Y, Lellouche J. Rapid identification of capsulated *Acinetobacter baumannii* using a density-dependent gradient test. BMC Microbiol **2020**; 20:285.
19. Smibert RM, Kreg NR. Phenotypic characterization. In: Gerhard P, Murray RG, Wood WA, and Krieg NR, eds. Methods for General and Molecular Bacteriology. Washington, D.C., USA: American Society for Microbiology, **1994**; 281–323.
20. Clemmer KM, Bonomo RA, Rather PN. Genetic analysis of surface motility in *Acinetobacter baumannii*. Microbiology (Reading) **2011**; 157:2534–44.
21. Curry A, Appleton H, Dowsett B. Application of transmission electron microscopy to the clinical study of viral and bacterial infections: present and future. Micron **2006**; 37:91–106.
22. Peleg AY, Jara S, Monga D, et al. *Galleria mellonella* as a model system to study *Acinetobacter baumannii* pathogenesis and therapeutics. Antimicrob Agents Chemother **2009**; 53:2605–9.
23. Kenyon JJ, Hall RM. Variation in the complex carbohydrate biosynthesis loci of *Acinetobacter baumannii* genomes. PLoS One **2013**; 8:e62160.
24. Kenyon JJ, Marzaioli AM, Hall RM, De Castro C. Structure of the K2 capsule associated with the KL2 gene cluster of *Acinetobacter baumannii*. Glycobiology **2014**; 24:554–63.
25. Brady MF, Jamal Z, Pervin N. Acinetobacter. In: Brady MF, Jamal Z, Pervin N, eds. Acinetobacter Treasure Island, FL: StatPearls Publishing; **2020**.
26. Bassetti M, Echols R, Matsunaga Y, et al. Efficacy and safety of cefiderocol or best available therapy for the treatment of serious infections caused by carbapenem-resistant gram-negative bacteria (CREDIBLE-CR): a randomised, open-label, multicentre, pathogen-focused, descriptive, phase 3 trial. Lancet Infect Dis. **In press**.
27. Dickstein Y, Leibovici L, Yahav D, et al; AIDA Consortium. Multicentre open-label randomised controlled trial to compare colistin alone with colistin plus meropenem for the treatment of severe infections caused by carbapenem-resistant gram-negative infections (AIDA): a study protocol. BMJ Open **2016**; 6:e009956.
28. de Breij A, Eveillard M, Dijkshoorn L, et al. Differences in *Acinetobacter baumannii* strains and host innate immune response determine morbidity and mortality in experimental pneumonia. PLoS One **2012**; 7:e30673.
29. Silva IN, Tavares AC, Ferreira AS, Moreira LM. Stress conditions triggering mucoid morphotype variation in *Burkholderia* species and effect on virulence in *Galleria mellonella* and biofilm formation in vitro. PLoS One **2013**; 8:e82522.
30. Ryall B, Carrara M, Zlosnik JE, et al. The mucoid switch in *Pseudomonas aeruginosa* represses quorum sensing systems and leads to complex changes to stationary phase virulence factor regulation. PLoS One **2014**; 9:e96166.
31. Lee H, Baek JY, Kim SY, et al. Comparison of virulence between matt and mucoid colonies of *Klebsiella pneumoniae* coproducing NDM-1 and OXA-232 isolated from a single patient. J Microbiol **2018**; 56:665–72.
32. Walker KA, Miner TA, Palacios M, et al. A *Klebsiella pneumoniae* regulatory mutant has reduced capsule expression but retains hypermucoviscosity. MBio **2019**; 10: 1–16.
33. McQueary CN, Kirkup BC, Si Y, et al. Extracellular stress and lipopolysaccharide modulate *Acinetobacter baumannii* surface-associated motility. J Microbiol **2012**; 50:434–43.
34. Hua X, Zhou Z, Yang Q, et al. Evolution of *Acinetobacter baumannii* in vivo: international clone II, more resistance to ceftazidime, mutation in ptk. Front Microbiol **2017**; 8:1256.
35. Roy R, You RI, Lin M Der, Lin NT. Mutation of the carboxy-terminal processing protease in *Acinetobacter baumannii* affects motility, leads to loss of membrane integrity, and reduces virulence. Pathogens. **In press**.
36. Tipton KA, Dimitrova D, Rather PN. Phase-variable control of multiple phenotypes in *Acinetobacter baumannii* strain AB5075. J Bacteriol **2015**; 197:2593–9.
37. Abdollahi S, Rasooli I, Mousavi Gargari SL. The role of TonB-dependent copper receptor in virulence of *Acinetobacter baumannii*. Infect Genet Evol **2018**; 60:181–90.
38. Ni T, Gilbert RJC. Repurposing a pore: highly conserved perforin-like proteins with alternative mechanisms. Philos Trans R Soc B Biol Sci **2017**; 372.
39. Rosado CJ, Kondos S, Bull TE, et al. The MACPF/CDC family of pore-forming toxins. Cell Microbiol **2008**; 10:1765–74.
40. Hamidian M, Hall RM. Genetic structure of four plasmids found in *Acinetobacter baumannii* isolate D36 belonging to lineage 2 of global clone 1. PLoS One **2018**; 13:e0204357.
41. Gu D, Dong N, Zheng Z, et al. A fatal outbreak of ST11 carbapenem-resistant hypervirulent *Klebsiella pneumoniae* in a Chinese hospital: a molecular epidemiological study. Lancet Infect Dis **2018**; 18:37–46.